

Cite this: *CrystEngComm*, 2012, 14, 7877–7881

www.rsc.org/crystengcomm

## COMMUNICATION

O $\cdots\pi$  and O–H $\cdots\pi$  interactions: the first disclosure of the nature of 1,3,4-oxadiazol $\cdots$ aromatic contacts†Li Wang,<sup>‡,ae</sup> Zhenfeng Zhang,<sup>‡,\*b</sup> Yibo Wang,<sup>c</sup> Yanbo Wu<sup>d</sup> and Shengyong Zhang<sup>\*,a</sup>

Received 31st July 2012, Accepted 12th September 2012

DOI: 10.1039/c2ce26224j

A new type of O $\cdots\pi$  interaction has been found and is rationalized by Møller–Plesset second-order perturbation theory calculations. LMOEDA energy decomposition reveals that it is mainly dominated by electrostatic and dispersion components; the origin of the electrostatic component is illustrated by the molecular electrostatic potential.

The ability of the  $\pi$ -cloud of benzene to act as a hydrogen bond acceptor has been shown both theoretically and experimentally.<sup>1</sup> In these cases, the phenyl  $\pi$ -cloud interacts with an electron-deficient atom, a hydrogen attached to an electronegative atom. As a general principle underlying hydrogen bond formation,<sup>2</sup> a strong hydrogen bond donor prefers to combine with a strong hydrogen bond acceptor, and a weak to pair off with a weak. Therefore, it is not surprising that a large number of C–H $\cdots\pi$  hydrogen bonds have been reported in recent times. By contrast, the O–H $\cdots\pi$  (as well as N–H $\cdots\pi$ ) hydrogen bonds involving benzene  $\pi$ -electrons are relatively scarce in the literature.<sup>3</sup>

The C $\cdots\pi$ , N $\cdots\pi$  and O $\cdots\pi$  interactions of the non-hydrogen bond type are even more scarce,<sup>4</sup> because unlike the H atom in the H $\cdots\pi$  system, C, N or O atoms are usually not sufficiently electron-deficient to serve as  $\pi$ -electron acceptors. However, the presence of strong electron-donating group(s) in the aromatic ring should lead to a substantial increase in  $\pi$ -electron density, thus the reinforced phenyl  $\pi$ -cloud may obtain the ability to interact with a non-hydrogen electron-deficient atom. In this situation, C $\cdots\pi$ , N $\cdots\pi$  and O $\cdots\pi$  interactions, though rare, can actually occur.<sup>4</sup>

Our interest in the 2-hydroxy-3-phenyl-3-[(5-phenyl-1,3,4-oxadiazol-2-yl)carbonyl]amino}propanoates stems from the fact

that compounds containing the 1,3,4-oxadiazole fragment have been identified to exhibit diverse biological activities,<sup>5</sup> and the properties are often closely related with the noncovalent interactions involving the 1,3,4-oxadiazole ring. In order to disclose the noncovalent interacting motifs preferred by the oxadiazole ring, we have synthesized a series of compounds of this kind, and examined their X-ray crystal structures.

Interestingly, we have discovered a new type of O $\cdots\pi$  interaction occurring between the oxadiazol oxygen and phenyl ring in methyl-(2*R*,3*S*)-2-hydroxy-3-phenyl-3-[(5-phenyl-1,3,4-oxadiazol-2-yl)-carbonyl]amino}propanoate, **1** (Fig. 1).<sup>6</sup> As is shown in Fig. 1, the oxadiazol atom O1\* lies above the C1–C6 ring; the distance of O1\* to the centroid is only 3.344(2) Å, which is markedly shorter than the upper limit of the sum of van der Waals radii, 3.42 Å (the phenyl ring half-thickness is taken as 1.7–1.9 Å).<sup>7</sup> The atom O1\*, we think, acts as a  $\pi$ -electron acceptor and the  $\pi$ -cloud of the C1–C6 ring acts as a  $\pi$ -electron donor. Despite a strong electron-withdrawing inductive effect, O1\* still exhibits

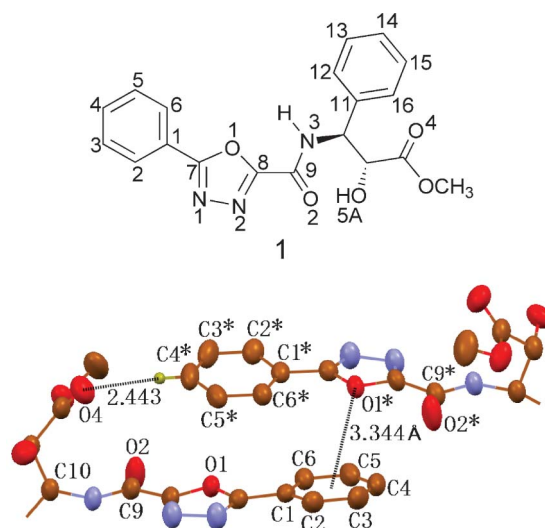


**Fig. 1** The partial packing diagram of **1**, showing the formation of a single O $\cdots\pi$  interaction between O1\* and the C1–C6 ring with an O $\cdots$ Cg distance of 3.344 Å (Cg is the centroid of the C1–C6 ring). For the sake of clarity, the C11–C16 ring and H atoms not involved in the motif shown have been omitted. Atoms marked with an asterisk (\*) are at the symmetry position: 1/2 + x, 1/2 – y, 1 – z.

<sup>a</sup>Department of Chemistry, School of Pharmacy, Fourth Military Medical University, Xian, P. R. China

<sup>b</sup>College of Chemistry and Chemical Engineering, Henan Normal University, Xinxiang 453007, P. R. China. E-mail: zzf5188@sohu.com; Fax: +86-373-3326336

<sup>c</sup>Department of Chemistry, Guizhou University, Key Laboratory of Guizhou High Performance Computational Chemistry, Guiyang 550025, P. R. China

<sup>d</sup>Institute of Molecular Science, Shanxi University, Taiyuan, 030006, Shanxi, P. R. China

<sup>e</sup>Department of Chemistry, School of Preclinical Medicine, Shanxi Medical University, 56 Xinjian, South Road, 030001 Tai Yuan, P. R. China

† CCDC 859574. For crystallographic data in CIF or other electronic format see DOI: 10.1039/c2ce26224j

‡ Z. Zhang and L. Wang contributed equally to this work.

relatively lower electron density due to its  $\pi$ -electron delocalization over the whole oxadiazol ring; the higher density of  $\pi$ -electrons on the oxadiazol ring is further delocalized over the bonded C1–C6 ring which possesses relatively low  $\pi$ -electron density, thus leading to a decrease in  $\pi$ -electron density on oxadiazol oxygen and an increase in electron density on the C1–C6 ring. The feature of charge distribution facilitates formation of the  $O\cdots\pi$  electrostatic interaction.

Recently, cation $\cdots\pi$  interactions, as typical representatives of electrostatic interactions, have been studied extensively by both experimentalists<sup>8–10</sup> and theorists.<sup>11–13</sup> The results shows that cation $\cdots\pi$  interactions were energetically favourable and energy minima were found when the cation is oriented along the principal axis of the ring.

The atom O1\* in compound **1**, however, deviates by 16.7° from being directly above the centre of the C1–C6 ring (Fig. 1). This large deviation is mainly attributed to the steric hindrance generated by the structural fragment bonded to C10, as well as the C4\*–H4\* $\cdots$ O4 interaction (H4\* $\cdots$ O4 = 2.44 Å and C4\*–H4\* $\cdots$ O4 = 159°). In addition, the steric hindrance and the C4\*–H $\cdots$ O4 interaction, also prevents C1\*–C6\* ring from forming an  $O\cdots\pi$  interaction with the O1 atom; the distance of O1 to C1\*–C6\* ring centroid is up to 3.675 Å.

If the above viewpoints are true, it should be probable to find a pair  $O\cdots\pi$  interactions in 2-phenyl-1,3,4-oxadiazole, where the steric factors and the C–H $\cdots$ O interaction are removed.

Keeping our motivation in mind, we replace C9 (Fig. 1) and the bonded structural fragment with a H atom to build the monomer and dimer of 2-phenyl-1,3,4-oxadiazole, the model system, for the evaluation of  $O\cdots\pi$  interactions. To accurately investigate the model system, a GGA-type density functional (WB97XD)<sup>14</sup> with long-range and semiempirical dispersion corrections was employed in combination with 6-311+G(d,p) basis set used to geometry optimization, and Møller–Plesset second-order perturbation theory MP2 with a large maug-cc-pvTZ<sup>15</sup> basis set including the basis set superposition error (BSSE) correction used to dimerization energy calculations. All the calculations were carried out by using GAUSSIAN 09<sup>16a</sup> and GAMESS<sup>16b</sup> packages. At the selected theoretical level, both the monomer and dimer of 2-phenyl-1,3,4-oxadiazole are found to be the energy minima. The optimized structures are shown in Fig. 2. As the figure shows, the core structure of the  $O\cdots\pi$  system has changed significantly with the substitution of bulky blocks with H atoms, and exhibits a pair of equivalent  $O\cdots\pi$  interactions along the principal axis. The O1 atom lies within 7° of being directly below the centroid of C1\*–C6\* ring, and the distance of O1 to the centroid is 3.328 Å. The dimer geometry is in very good accordance with what we expected. The total dimerization energy is  $-11.87$  kcal mol<sup>-1</sup>, showing that the  $O\cdots\pi$  interaction is thermodynamically favorable. The results validates our foregoing hypothesis that the steric hindrance does prevent O1 from forming an efficient  $O\cdots\pi$  interaction with the C1\*–C6\* ring in **1**, and have also presented compelling evidence that  $O\cdots\pi$  interaction(s) can actually occur between phenyl ring and 1,3,4-oxadiazol oxygen atom despite presence of steric hindrance in some cases.

To clarify the nature of the  $O\cdots\pi$  interaction, we employed the localized molecular orbital energy decomposition analysis (LMOEDA) approach of Su and Li<sup>17</sup> to decompose the  $O\cdots\pi$  interaction energy into electrostatic, exchange, repulsion,

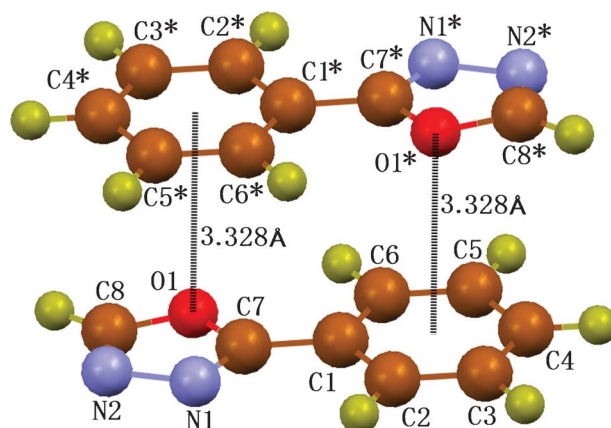


**Fig. 2** The dimeric structure of 2-phenyl-1,3,4-oxadiazole optimized at WB97XD/6-311+G(d,p) level, showing the formation of a pair of equivalent  $O\cdots\pi$  interactions.

polarization, and dispersion components. The LMOEDA computations are performed in GAMESS at the MP2/maug-cc-pVTZ level,<sup>15</sup> and the results are summarized in Table 1. As the table shows, the  $O\cdots\pi$  interaction is mainly dominated by two components: dispersion energy and electrostatic energy, which contribute 62% and 31%, respectively, to the total dimerization energy ( $-11.87$  kcal mol<sup>-1</sup>).

We have also calculated and analyzed the electrostatic potential (ESP) of the 2-phenyl-1,3,4-oxadiazole monomer to further probe the origin of the electrostatic component. It is well known that there is a negative ESP above the centroid of the C1–C6 ring. For  $O\cdots\pi$  electrostatic bonding, the oxadiazole oxygen is expected to show a positive ESP value for complementarity to the benzene ring. Fig. 3 confirms this expectation showing positive ESP for the oxadiazole oxygen. The electrostatic potential features are well supported by the DFT-based Mulliken population analysis. The representative result of charge distribution is illustrated in Fig. 4. As can be seen from the figure, among all the oxadiazole ring atoms, the atom O1 carries the largest Mulliken positive charge (+0.157), and the benzene ring as a whole (not including hydrogens) carries highest negative charge ( $-1.152$ ). Thus, the features in electrostatic potential and charge distribution have well clarified the origin of the electrostatic component of the  $O\cdots\pi$  interaction. Though the electrostatic interaction does not solely dominate the total interaction energy, the result validates our foregoing hypothesis that the oxadiazole oxygen in compound **1** exhibits relatively lower electron density due to its  $\pi$ -electron delocalization.

In order to further probe the generality of the  $O\cdots\pi$  interaction in aromatic 1,3,4-oxadiazoles, we conducted a systematic search of the CSD for structures that match the fragment shown in Scheme 1. The two restrictions applied were that the distance ( $d$ )

**Table 1** LMOEDA binding energy decomposition at MP2/maug-cc-pVTZ level (kcal mol<sup>-1</sup>)<sup>a</sup>

$\Delta E^{\text{ele}}$	$\Delta E^{\text{ex+rep}}$	$\Delta E^{\text{disp}}$	$\Delta E^{\text{pol}}$	$\Delta E^{\text{cp}}$
-8.34	15.23	-16.86	-1.91	-11.87

<sup>a</sup> ele = electrostatic, ex = exchange, rep = repulsion, disp = dispersion, pol = polarization, and cp = total.

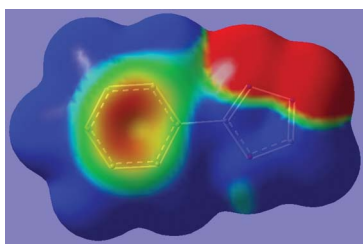


**Fig. 3** MP2/maug-pp-pVTZ electrostatic potential for the 2-phenyl-1,3,4-oxadiazole monomer. The blue region represents the positive part of the electrostatic potential, and the red region the negative part of the electrostatic potential.

between the centroid of phenyl ring and the oxadiazol oxygen atom be equal or less than 3.76 Å and that the angle,  $\alpha$ , defined by the vector perpendicular to the phenyl ring and the vector passing through the centroid to the oxygen atom, be equal or less than 20°. The 3.76 Å cut-off was chosen based on the van der Waals radius of oxygen, taken as 1.52 Å, and the phenyl ring half-thickness of 1.7–1.9 Å.<sup>7</sup> The liberal value of 3.76 Å was calculated as 1.52 + 1.9 plus 10%, to capture all potential O $\cdots\pi$  interactions. This search gave a total of 86 hits; these hits were scrutinized manually to exclude those obviously inappropriate compounds including disordered and polymorphic structures, and aggregates encapsulated within obvious hydrogen bonding which presumably takes precedence over a supposed O $\cdots\pi$  interaction. Under these constraints, 50 crystal structures remained, representing a total of 109 unambiguous O $\cdots\pi$  interactions (Table 2). Inspection of these structures revealed: (i) no specific mention of the interactions was made in previous work and (ii) the majority of O $\cdots\pi$  systems exhibit the expected geometry for the O $\cdots\pi$  interactions (Fig. 2), whereas some others exhibit relatively large interacting geometry due to steric hindrance. The results have confirmed that O $\cdots\pi$  interactions do exist widespread in aromatic 1,3,4-oxadiazoles despite the presence of steric hindrance.

Given that O $\cdots\pi$  interactions occur universally in phenyl-substituted 1,3,4-oxadiazoles, it is possible to find similar O $\cdots\pi$  interactions in 5-phenylfuran derivatives, and the O $\cdots\pi$  interactions there are expected to be weaker. In view of this, we also conducted a systematic study of such compounds in the CSD, and interestingly found that the furan oxygen actually makes a close approach to the adjacent phenyl ring along the principal axis; the average distance of oxygen to the phenyl ring centroid is 3.46 Å and the average angle is 12.9° (Table 3). The result reveals that

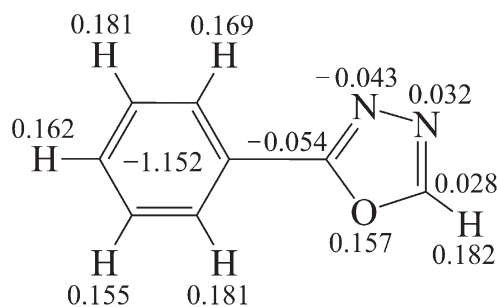
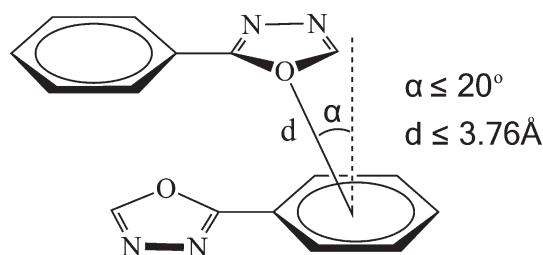


**Fig. 4** Charge distribution of 2-phenyl-1,3,4-oxadiazole in the optimized dimer (calculated at the WB97XD/6-311+G(d,p) level, and the no. of the atom is the same as shown in Fig. 2).



**Scheme 1** Geometric parameters defining the O $\cdots\pi$  interactions covered in this work.

O $\cdots\pi$  interactions also exist in furan derivatives, but they are weaker than those in phenyl-substituted 1,3,4-oxadiazoles.

This kind of O $\cdots\pi$  interaction, despite its widespread existence, is not reported so far in the literature. Though a number of O $\cdots\pi$  interactions have been reported recently,<sup>18</sup> their nature is nothing but a lone-pair (lp) $\cdots\pi$  interaction. In aryl 1,3,4-oxadiazoles, the O $\cdots\pi$  interaction occurs between the electron-deficient oxadiazol oxygen and the  $\pi$ -electron-rich phenyl ring, distinctly not a lp $\cdots\pi$  interaction.

We have also probed the vibrational characteristics of the oxadiazole ring in **1** in an attempt to observe this interaction in solution. IR spectroscopic measurements of the stretching frequency of the oxadiazole in the crystalline material and in solutions of acetone and acetonitrile did not show any dramatic changes. The FTIR spectra of the crystalline sample in KBr showed the characteristic vibrations at 1548 cm<sup>-1</sup>. In acetone and acetonitrile, there was no appreciable shift in stretching frequency of the oxadiazole ring. However, a moderate red shift (1544 cm<sup>-1</sup>) was observed in CH<sub>2</sub>Cl<sub>2</sub>, maybe due to formation of a competitive Cl $\cdots\pi$  interaction.<sup>19</sup> The result indicates that the O $\cdots\pi$  interaction in **1** has an effect on the stretching vibration of the oxadiazole, but this effect is considerably minimal.

Additionally, the hydroxyl O5–H5A in compound **1** could have formed a conventional intramolecular H bond to the carbonyl O4 (Fig. 5), however, the hydroxyl atom H5A points not to the O4 atom but to the intermolecular C11\*–C16\* ring centroid of the neighboring translation-related molecule, the distances H5A $\cdots$ Cg and O5 $\cdots$ Cg being 2.69 and 3.460(2) Å, respectively, and the H-bond angle 161°. Hence, the O–H $\cdots\pi$  interaction has all the geometrical attributes of a hydrogen bond.<sup>20</sup> In view of an offset of

**Table 2** Result of database analysis of O $\cdots\pi$  interactions in phenyl-substituted 1,3,4-oxadiazoles

O $\cdots\pi$ interactions	No. of entries	Mean geometric parameters	
		$d^b/\text{Å}$	$\alpha^c/^\circ$
	50 <sup>a</sup>	3.41	9.5

<sup>a</sup> Refcodes: COVHOL, DAXBOU, EDOTAT, FEQNAR, LARNOI, LEQPON, LEQPUT, NAXDIZ, NEVXIW, NEXHUU, QUJNUF, QUJPER, QUJPOB, REYZOL, SUHWEY, WEPJUX, XOXLAX, YETSLA, YETSOB, ADEKOJ, COZJOR, DAXBUA, GIKYOP, GUPYUM, HAXTAC, HAXTEG, JARBOU, JOLDAP, LARMUN, LODZUZ, MOMNAE, NEVXOC, NILQAB, OBUJEB, OIXGUA, OJIFES, PUMGAG, QUVPON, RAXROY, REYZUR, SABPIV, TUCYAS, TUHXID02, VAXYEZ, WEDWUY, WEHQUW, WEKSAH, WONJOZ, XIWRIF, XOZHAW.<sup>b</sup> The distance from the oxadiazol oxygen to the phenyl ring centroid. <sup>c</sup> The angle between the oxadiazol oxygen-phenyl ring centroid vector and the vector perpendicular to the phenyl ring.



**Table 3** Result of database analysis of O $\cdots\pi$  contacts in 5-phenyl-furan derivatives

O $\cdots\pi$ interactions	No. of entries	Mean geometric parameters	
		$d^b/\text{\AA}$	$\alpha^c/^\circ$
	5 <sup>a</sup>	3.46	12.9

<sup>a</sup> Refcodes: WULVEF, NUKWUL, TIBBIQ, DUDWUY, KOKMON. <sup>b</sup> The distance from the furan oxygen to the phenyl ring centroid. <sup>c</sup> The angle between the furan oxygen-phenyl ring centroid vector and the vector perpendicular to the phenyl ring.

only 0.543 Å of H5A with respect to the C11\*–C16\* centroid, the O–H $\cdots\pi$  bond is classed as “centroid type”.

The O–H $\cdots\pi$  H bonds of the “centroid type” are uncommon in the literature, especially in organic molecules.<sup>3a,b</sup> Some O–H $\cdots\pi$  hydrogen bonds have been reported recently,<sup>3c,g</sup> however, they belong to the “edge type”, where the O–H group makes a close approach to only two adjacent carbons of a particular phenyl group.

The crystal structure of **1** also exhibits two intramolecular N–H $\cdots$ N and C–H $\cdots$ O hydrogen bonds (Fig. 5); the distances N3–H $\cdots$ N2 and C6–H $\cdots$ O1 are 2.46 and 2.54 Å, respectively, and the angles 106 and 100°, respectively. The two H bonds collaboratively maintain a planar conformation to the [(5-phenyl-1,3,4-oxadiazol-2-yl)carbonyl]amino fragment, thus allowing  $\pi$ -electrons to localize sufficiently between the oxadiazole and C1–C6 ring. This sets the stage for the foregoing O $\cdots\pi$  interaction. The crystallographic data are presented in Table 4.

In addition to the O–H $\cdots\pi$  and O $\cdots\pi$  interactions, there are three intermolecular H bonds in **1**, one of C–H $\cdots$ N, and two of C–H $\cdots$ O type. The distances C12–H12 $\cdots$ N1, C16–H16 $\cdots$ O2 and C5–H5 $\cdots$ O3 are 2.54, 2.50 and 2.68 Å, respectively, and the corresponding angles 177, 144 and 157°, respectively. These noncovalent interactions synergistically constitute a 3D structure. Considering no conventional hydrogen bonds involved in **1**, we think the O $\cdots\pi$  interaction not only plays a crucial role in the specific packing motif of aryl-1,3,4-oxadiazoles, but also may be of

**Table 4** Crystallographic data for **1**<sup>a</sup>

Compound	<b>1</b>
Formula	C <sub>19</sub> H <sub>15</sub> N <sub>3</sub> O <sub>5</sub>
$M_r$	367.36
Crystal system	Orthorhombic
Space group	$P2_12_12_1$
$a/\text{\AA}$	6.796(2)
$b/\text{\AA}$	11.993(3)
$c/\text{\AA}$	21.790(5)
$V/\text{\AA}^3$	1775.9(7)
$Z$	4
$d/\text{g cm}^{-3}$	1.374
$\mu/\text{mm}^{-1}$	0.101
$\lambda/\text{\AA}$	0.71073
Crystal dimensions/ $\text{mm}^{-3}$	0.18 $\times$ 0.29 $\times$ 0.39
Reflections measured	8686
Independent reflections	3080
$(R_{\text{int}} \sim 0.025)$	
Final $R$	0.0246
$wR_2$ (for all reflections)	0.0638

<sup>a</sup> Crystallization from ethyl acetate by slow evaporation in air yields colorless block crystals. SADABS absorption correction. Standard crystallographic computations (refinement on  $F^2$  of all reflections). Data/restraints/parameters = 3080/0/253. Data collected on the Bruker–Nonius, SMART CCD detector.

great importance to understanding their biochemical and physical behaviours.

In conclusion, in-depth structural studies have revealed a new type of O $\cdots\pi$  interaction occurring in aromatic 1,3,4-oxadiazoles. *Ab initio* computations performed at the WB97XD/6-311+G(d,p) level provided effective support to the interaction. LMOEDA binding energy decomposition at the MP2/maug-cc-pVTZ level has shown that although the dispersion component makes the largest contribution to the O $\cdots\pi$  interaction, the electrostatic component may be more important in controlling the directionality and geometrical details of the interaction. Therefore, its origin has been accounted for by molecular electrostatic potential and Mulliken population analysis. The present work, we believe, may be the first disclosure of the nature of 1,3,4-oxadiazol $\cdots$ aromatic contacts.

## References

- (a) W. G. Read, E. J. Campbell and G. Henderson, *J. Chem. Phys.*, 1983, **78**, 3501; (b) F. A. Balocchi, J. H. Williams and W. Klemperer, *J. Phys. Chem.*, 1983, **87**, 2079; (c) S. Suzuki, P. G. Green, R. E. Bumgarner, S. Dasgupta, W. A. Goddard III and G. A. Blake, *Science*, 1992, **257**, 942; (d) D. A. Rodham, S. Suzuki, R. D. Suenram, F. J. Lovas, S. Sagupta, W. A. Goddard III and G. A. Blake, *Nature*, 1993, **362**, 735.
- M. C. Etter, *Acc. Chem. Res.*, 1990, **23**, 120–126.
- (a) J. L. Atwood, F. Hamada, K. D. Robinson, G. W. Orr and R. L. Vincent, *Nature*, 1991, **349**, 683–684; (b) G. Ferguson and J. F. Gallagher, *Acta Crystallogr., Sect. C: Cryst. Struct. Commun.*, 1994, **50**, 70–73; (c) P. Kus and P. G. Jones, *Z. Naturforsch., Teil B*, 2004, **59**, 1026; (d) M. Nanjo, K. Matsudo and K. Mochida, *Inorg. Chem. Commun.*, 2003, **6**, 1065–1068; (e) J.-H. Yang, W. Li, S.-L. Zheng, Z.-L. Huang and X.-M. Chen, *Aust. J. Chem.*, 2003, **56**, 1175–1178; (f) S. Apel, S. Nitsche, K. Beketov, W. Seichter, J. Seidel and E. Weber, *J. Chem. Soc., Perkin Trans. 2*, 2001, 1212–1218; (g) N. M. Deschamps, J. H. Kaldis, P. E. Lock, J. F. Britten and M. J. McGlinchey, *J. Org. Chem.*, 2001, **66**, 8585–8591; (h) V. Cody and J. Hazel, *Acta Crystallogr., Sect. B: Struct. Crystallogr. Cryst. Chem.*, 1977, **33**, 3180–3184.
- (a) Z. Zhang, Y. Wu and G. Zhang, *CrystEngComm*, 2011, **13**, 4496–4499; (b) Z. Zhang, H. Tong, Y. Wu and G. Zhang, *New J. Chem.*, 2012, **36**, 44–47.

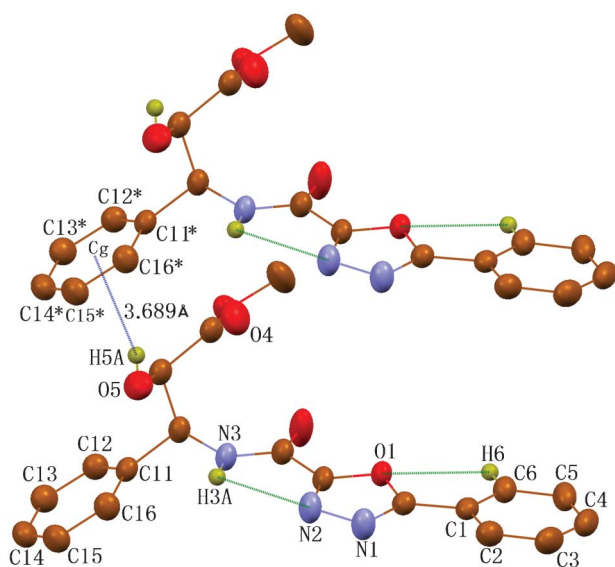


**Fig. 5** Partial packing diagram of **1**, showing the formation of one intermolecular O–H $\cdots\pi$  and two intramolecular N–H $\cdots$ N and C–H $\cdots$ O hydrogen bonds. Symmetry code: 1 +  $x$ ,  $y$ ,  $z$ .

- 5 (a) E. A. Musad, R. Mohamed, B. A. Saeed, B. S. Vishwanath and K. M. L. Rai, *Bioorg. Med. Chem. Lett.*, 2011, **21**, 3536–3540; (b) X. Zheng, Z. Li, Y. Wang, W. Chen, Q. Huang, C. Liu and G. Song, *J. Fluorine Chem.*, 2003, **123**, 163–169.
- 6 Synthesis of **1**: A mixture of ethyl 5-phenyl-1,3,4-oxadiazole-2-carboxylate (0.013 mol) and (2*R*,3*S*)-methyl 3-amino-2-hydroxy-3-phenylpropanoate (0.016 mol) in toluene is heated under reflux for 24 hours. After disappearance of ethyl 5-phenyl-1,3,4-oxadiazole-2-carboxylate by TLC, the residue obtained by evaporation of solvent is purified by column chromatography using a binary solvent mixture of petroleum ether (60–90)–ethyl acetate (3 : 1).
- 7 C. Janiak, *J. Chem. Soc., Dalton Trans.*, 2000, 3885–3896.
- 8 (a) D. K. Chakravorty, B. Wang, M. N. Ucisik and K. M. Merz, *J. Am. Chem. Soc.*, 2011, **133**, 19330–19333; (b) J. C. Maa and D. A. Dougherty, *Chem. Rev.*, 1997, **97**, 1303–1324.
- 9 P. Lakshminarasimhan, R. B. Sunoj, J. Chandrasckhar and V. Ramamurthy, *J. Am. Chem. Soc.*, 2000, **122**, 4815–4816.
- 10 Y. V. Nelyubina, P. Y. Barzilovich, M. Y. Antipin, S. M. Aldoshin and K. A. Lyssenko, *ChemPhysChem*, 2011, **12**, 2895–2898.
- 11 R. A. Kumpf and D. A. Dougherty, *Science*, 1993, **261**, 1708–1710.
- 12 S. Mecozzi, A. P. West and D. A. Dougherty, *J. Am. Chem. Soc.*, 1996, **118**, 2307–2308.
- 13 J. W. Caldwell and P. A. Kollman, *J. Am. Chem. Soc.*, 1995, **117**, 4177–4178.
- 14 (a) S. Grimme, *J. Comput. Chem.*, 2006, **27**, 1787–1799; (b) J.-D. Chai and M. Head-Gordon, *Phys. Chem. Chem. Phys.*, 2008, **10**, 6615–6620.
- 15 (a) H He Li Be B C N O F Ne Na Mg Al Si P S Cl Ar: E. Papajak and D. G. Truhlar, *J. Chem. Theory Comput.*, 2010, **6**, 597–601; (b) B-F: R. A. Kendall, T. H. Dunning Jr. and R. J. Harrison, *J. Chem. Phys.*, 1992, **96**, 6796–6806.
- 16 (a) M. J. Frisch, G. W. Trucks, H. B. Schlegel, G. E. Scuseria, M. A. Robb, J. R. Cheeseman, G. Scalmani, V. Barone, B. Mennucci, G. A. Petersson, H. Nakatsuji, M. Caricato, X. Li, H. P. Hratchian, A. F. Izmaylov, J. Bloino, G. Zheng, J. L. Sonnenberg, M. Hada, M. Ehara, K. Toyota, R. Fukuda, J. Hasegawa, M. Ishida, T. Nakajima, Y. Honda, O. Kitao, H. Nakai, T. Vreven, J. A. Montgomery, Jr., J. E. Peralta, F. Ogliaro, M. Bearpark, J. J. Heyd, E. Brothers, K. N. Kudin, V. N. Staroverov, R. Kobayashi, J. Normand, K. Raghavachari, A. Rendell, J. C. Burant, S. S. Iyengar, J. Tomasi, M. Cossi, N. Rega, J. M. Millam, M. Klene, J. E. Knox, J. B. Cross, V. Bakken, C. Adamo, J. Jaramillo, R. Gomperts, R. E. Stratmann, O. Yazyev, A. J. Austin, R. Cammi, C. Pomelli, J. Ochterski, R. L. Martin, K. Morokuma, V. G. Zakrzewski, G. A. Voth, P. Salvador, J. J. Dannenberg, S. Dapprich, A. D. Daniels, O. Farkas, J. B. Foresman, J. V. Ortiz, J. Cioslowski and D. J. Fox, *GAUSSIAN 09 (Revision A.2)*, Gaussian, Inc., Wallingford, CT, 2009; (b) M. W. Schmidt, K. K. Baldridge, J. A. Boatz, S. T. Elbert, M. S. Gordon, J. H. Jensen, S. Koseki, N. Matsunaga, K. A. Nguyen, S. Su, T. L. Windus, M. Dupuis and J. A. Montgomery, *J. Comput. Chem.*, 1993, **14**, 1347–1363.
- 17 P. Su and H. Li, *J. Chem. Phys.*, 2009, **131**, 014102.
- 18 (a) J. E. Gautrot, P. Hodge, D. Cupertino and M. Helliwell, *New J. Chem.*, 2006, **30**, 1801–1807; (b) A. Galstyan, P. J. S. Miguel and B. Lippert, *Chem.–Eur. J.*, 2010, **16**, 5577–5580; (c) S. R. Choudhury, P. Gamez, A. Robertazzi, C. Y. Chen, H. M. Lee and S. Mukhopadhyay, *Cryst. Growth Des.*, 2008, **8**, 3773–3784; (d) S. K. Seth, B. Dey, T. Kar and S. Mukhopadhyay, *J. Mol. Struct.*, 2010, **973**, 81–88; (e) C. Biswas, M. G. B. Drew, D. Escudero, A. Frontera and A. Ghosh, *Eur. J. Inorg. Chem.*, 2009, 2238–2246.
- 19 (a) G.-G. Hou, J.-P. Ma, T. Sun, Y.-B. Dong and R.-Q. Huang, *Chem.–Eur. J.*, 2009, **15**, 2261–2265; (b) E. Ye, Y.-W. Zhang, H. Wang, Y.-Y. Niu and S. W. Ng, *Acta Crystallogr., Sect. E: Struct. Rep. Online*, 2006, **62**, o2594–o2595; (c) L.-F. Shi, Y. Li, Z. Si, Y. Guan and H. Cao, *Acta Crystallogr., Sect. E: Struct. Rep. Online*, 2010, **67**, m9–m10.
- 20 (a) R. Taylor and O. Kennard, *J. Am. Chem. Soc.*, 1982, **104**, 5063–5070; (b) G. A. Jeffrey and W. Saenger, *Hydrogen Bonding in Biological Structures*, Springer-Verlag, Berlin, 1991.